

Extended state observer-based control with an adjustable parameter for a large ground-based telescope

Xiao-Xia Yang, Yong-Ting Deng, Bin Zhang and Jian-Li Wang

Changchun Institute of Optics, Fine Mechanics and Physics, Chinese Academy of Sciences, Changchun 130033, China;
yxxair@163.com, dyt0612@163.com

Received 2021 August 23; accepted 2021 September 28

Abstract The high-precision requirements will always be constrained due to the complicated operating conditions of the ground-based telescope. Owing to various internal and external disturbances, it is necessary to study a control method, which should have a good ability on disturbance rejection and a good adaptability on system parameter variation. The traditional proportional-integral (PI) controller has the advantage of simple and easy adjustment, but it cannot deal with the disturbances well in different situations. This paper proposes a simplified active disturbance rejection control law, whose debugging is as simple as the PI controller, and with better disturbance rejection ability and parameter adaptability. It adopts a simplified second-order extended state observer (ESO) with an adjustable parameter to accommodate the significant variation of the inertia during the different design stages of the telescope. The gain parameter of the ESO can be adjusted online with a recursive least square estimating method once the system parameter has changed significantly. Thus, the ESO can estimate the total disturbances timely and the controller will compensate them accordingly. With the adjustable parameter of the ESO, the controller can always achieve better performance in different applications of the telescope. The simulation and experimental verification of the control law was conducted on a 1.2-meter ground based telescope. The results verify the necessity of adjusting the parameter of the ESO, and demonstrate better disturbance rejection ability in a large range of speed variations during the design stages of the telescope.

Key words: extended state observer — large ground based telescope — recursive least square — disturbance rejection

1 INTRODUCTION

Larger and larger aperture ground-based telescopes have been required to meet the rapid development of the deep space exploration technology. Hence, the corresponding higher accuracy control law should be studied to satisfy the high-precision detection requirements of the large telescope. The main axis control of the large ground based telescope has confronted the following key challenges in the engineering practice.

(i) Due to the complicated operating conditions of the ground based telescope, the ultimate imaging accuracy will be easily affected by various internal and external disturbances (Song et al. 2021) such as friction torque, motor torque ripple, parameter perturbations, un-modeled dynamics, wind torque, earth vibration, load change, etc.

These disturbances may degrade the final imaging quality badly if the controller does not reject them adequately.

(ii) For the large ground based telescope, the total load inertia is very large, which will result in a relatively low resonance frequency of the mechanical structure. This will limit the bandwidth of the controller design.

(iii) Since the inertia of the main axis will change greatly during the design process of the telescope, the controller should be designed to accommodate this variation adaptively. Primarily, a more robust controller with high control precision should be studied to meet the high precision imaging requirements of ground-based telescopes. Moreover, the simpler designing and easier debugging controller is more favorable to engineers in the engineering practice. Therefore, the proposed controller should not be too complicated to implement.

To handle the problems encountered in engineering, many improved control methods have been developed, such as the disturbance observer-based control (Back & Kim 2015), variable structure PID control (Jafarov et al. 2005), fuzzy neural control (Chen et al. 2016), adaptive compensation control (Rigatos 2009), acceleration feedback control (Wang et al. 2016) and sliding mode control (Xian-qi et al. 2019) etc. In one way, these controllers can improve the control characteristics of the system in certain aspects such as mediating the contradiction of rapidness and the overshoot, estimating and compensating the mixed disturbances, etc.

Active Disturbance Rejection Controller (ADRC) (Han 2009) has demonstrated a good dynamic performance in the presence of large kinds of uncertainties in various areas of application, such as mechatronic systems (Alonge et al. 2017; Shi et al. 2017; Yao et al. 2020), fluidized bed combustor (Wu et al. 2020), flight control system (Xue et al. 2015), flywheel energy storage system (Chang et al. 2015), pneumatic muscle actuator system (Yuan et al. 2019), tracked vehicles system (Xia et al. 2018), et al. In this paper, we pay particular attention to a simplified structure of ADRC, which uses the disturbance rejection idea of ADRC but does not apply the whole structure indiscriminately. The method will be implemented and tuned as easily as a proportional-integral (PI) controller (Ang et al. 2005) and has better robustness and higher control accuracy. Actually, the design of the ADRC is not completely model-independent (Huang & Xue 2014). The appropriate prior knowledge of the control gain b of the extended state observer (ESO) is needed in the controller design. It indicates that the variation of b has a significant effect on the stability of ADRC (Wu & Chen 2009). The experience reveals that a more accurate parameter b can result in a quicker convergence rate and higher control accuracy of a real-time system.

In this paper, a simple identification method will be proposed, which can be implemented easily online. Then a simplified ADRC controller will be given in detail. The proposed algorithm demonstrates a good performance on the main axis control of a 1.2-m telescope driven by DC motors.

2 PROBLEM STATEMENTS

2.1 Mathematical Models of the System

The ideal linear model of the DC motor can be described as follows

$$\begin{cases} \dot{i} = -R_a i/L_a + u/L_a - K_e v/L_a \\ \dot{v} = (K_m i + T_d)/J. \end{cases} \quad (1)$$

where i is the current, u is the voltage, L_a is the electrical inductance, R_a is the electrical resistance, J is the equivalent motor and load inertia, K_m is the motor torque constant, T_d is the total torque disturbance, K_e is the back electromotive coefficient, and v is the angular speed. From Equation (1) we get the following second order system

$$L_a \ddot{v}/R_a + \dot{v} + K_m K_e v/(J R_a) - K_m u/(J R_a) - T_d/J = 0. \quad (2)$$

According to the electrical properties of the DC motor used for the main axis, we have $L_a/R_a \ll 1$, which means that the coefficient of \dot{v} is significantly larger than \ddot{v} . Therefore, the mathematical model of the system can be simplified as the following first-order system, where the item $L_a \ddot{v}/R_a$ is neglected.

$$\dot{v} = -K_m K_e v/(J R_a) + K_m u/(J R_a) + T_d/J. \quad (3)$$

The core of ADRC is the ESO (Hui et al. 2020; Liu et al. 2019), which can be used to estimate the lumped uncertainties with the input and output signals of the system. From Equation (3), a second-order ESO can be designed where the control gain is $b = K_m/(J R_a)$. As parameter b has no intuitive physical significance, it will be treated as a dimensionless parameter in the subsequent discussion. The control gain b has a close relationship with the inertia of the system. Therefore it will change significantly with the change of the telescope structure.

2.2 Estimation of Control Gain b

For the above mentioned system, numerous simulations show that if the relative error for estimating parameter b is less than 30%, it will not affect the control characteristic distinctly. That is:

$$|(b - b_0)/b| \leq 30\%, \quad (4)$$

where b_0 is the estimated value of b . Notice that the control gain b in Equation (3) is related to the equivalent load inertia J of the system which will change significantly with the load variation during different design stages of the telescope. The controller will produce poor results if there is a significant change of parameter b . To maintain good performance of the ESO, we need to re-estimate parameter b when it changes significantly.

2.2.1 The multiple open-loop (MOL) experiment method

The commonly used method for estimating parameter b in engineering practice is the multiple open-loop (MOL) method. It conducts several open-loop experiments, which



Fig. 1 Block diagram of the open-loop.

use the constant voltage $u_k, k = 1, \dots, n$, as the input and result in the corresponding output v_k for the k^{th} experiment. Figure 1 gives the block diagram of the open-loop experiment. Without loss of generality, the disturbance torque T_d will be simplified as a constant torque related to the sign of the control input u , that is $T_d = -\text{sgn}(u)C_{T_d}$, where C_{T_d} is a constant. Suppose $\alpha_1 = -K_m K_e / (JR_a)$, $\alpha_2 = C_{T_d} / J$, then Equation (3) can be expressed as:

$$\dot{v} = \alpha_1 v + bu - \alpha_2 \text{sgn}(u). \quad (5)$$

By solving Equation (5) we can get:

$$v_k(t) = \frac{be^{\alpha_1 t} - b}{\alpha_1} \left(u_k - \frac{\alpha_2 \text{sgn}(u_k)}{b} \right), \quad (6)$$

where $v_k(t)$ represents the speed output corresponding to the control input u_k . Notice that $\alpha_1 < 0$, therefore

$$\lim_{t \rightarrow +\infty} v_k(t) = -\frac{b}{\alpha_1} \left(u_k - \frac{\alpha_2 \text{sgn}(u_k)}{b} \right). \quad (7)$$

Let $\lambda = \begin{bmatrix} -\frac{b}{\alpha_1} \\ \frac{\alpha_2}{\alpha_1} \end{bmatrix}$, $\psi = \begin{bmatrix} \lim_{t \rightarrow +\infty} v_1(t) \\ \vdots \\ \lim_{t \rightarrow +\infty} v_n(t) \end{bmatrix}$, $A = \begin{bmatrix} u_1 & \text{sgn}(u_1) \\ \vdots & \vdots \\ u_n & \text{sgn}(u_n) \end{bmatrix}$, then, Equation (7) can be expressed as

$$\psi = A\lambda. \quad (8)$$

Using the least square method, the estimate of parameter λ is

$$\tilde{\lambda} = (A^T A)^{-1} A^T \psi. \quad (9)$$

Furthermore, notice that

$$v_k \left(-\frac{1}{\alpha_1} \right) = \frac{be^{-1} - b}{\alpha_1} \left(u_k - \frac{\alpha_2 \text{sgn}(u_k)}{b} \right) = 0.632 \lim_{t \rightarrow +\infty} v_k(t). \quad (10)$$

That is $-\frac{1}{\alpha_1}$ is the time point t_k , which satisfies

$$v_k(t_k) = 0.632 \lim_{t \rightarrow +\infty} v_k(t). \quad (11)$$

Then the estimate value of α_1 should be

$$\tilde{\alpha}_1 = \left(-\sum_{k=1}^n \frac{1}{t_k} \right) / n. \quad (12)$$

Hence the estimated value of parameter b is

$$\tilde{b} = -\tilde{\lambda}_1 / \tilde{\alpha}_1, \quad (13)$$

where $\tilde{\lambda}_1$ is the first term of $\tilde{\lambda}$. Figure 2 shows the results of the MOL experiments on a 1.2-m aperture telescope. From the data cursor text string in Figure 2, we get

$$\psi = \begin{bmatrix} 3.10 \\ 6.23 \\ 9.28 \\ 11.26 \end{bmatrix} \times \pi / 180, \quad A = \begin{bmatrix} 9.6 & 1 \\ 14.4 & 1 \\ 19.2 & 1 \\ 24.0 & 1 \end{bmatrix},$$

$$\begin{bmatrix} t_1 \\ t_2 \\ t_3 \\ t_4 \end{bmatrix} = \begin{bmatrix} 2.52 \\ 2.50 \\ 2.30 \\ 2.22 \end{bmatrix},$$

then the parameter b can be calculated according to Equations (9), (11), (12) and (13), where $b = 2.37 \times 10^{-2}$.

Above all, the MOL method needs more than one open-loop experiment and the data analysis should be done off-line. To achieve a steady value of the angular speed, the MOL method needs longer time with larger angular position variation which may break the mechanical limits of the main axis (usually the mechanical limits for the altitude axis are $0^\circ \sim 90^\circ$).

2.2.2 The recursive least square (RLS) method

In this paper, a simpler recursive least square (RLS) identification method, which exhibits a better quality than the MOL method will be given. Equation (5) can be discretized as follows using the forward Euler method

$$v_{k+1} = (1 + \alpha_1 T_s) v_k + b T_s u_k - \alpha_2 T_s \text{sgn}(u_k), \quad (14)$$

where T_s is the sampling period. Let $\phi_k = [v_k \ u_k \ -\text{sgn}(u_k)]^T$, $\eta = [1 + \alpha_1 T_s \ b T_s \ \alpha_2 T_s]^T$ then Equation (14) can be expressed as the following Auto-regression with extra input (ARX) model

$$v_{k+1} = \eta^T \phi_k. \quad (15)$$

Thus, the RLS method can be applied to estimate parameter η as follows

$$\tilde{\eta}_{k+1} = \tilde{\eta}_k + \beta_k P_k \phi_k (v_{k+1} - \tilde{\eta}_k^T \phi_k), \quad (16)$$

where $\tilde{\eta}_k$ means the k^{th} estimate value for η . P_k and β_k are defined as follows

$$P_k = \left(\sum_{i=0}^k \phi_i \phi_i^T \right)^{-1}, \quad \beta_k = (1 + \phi_k^T P_k \phi_k)^{-1}. \quad (17)$$

The recursive expression for P_k is

$$P_{k+1} = P_k - \beta_k P_k \phi_k \phi_k^T P_k. \quad (18)$$

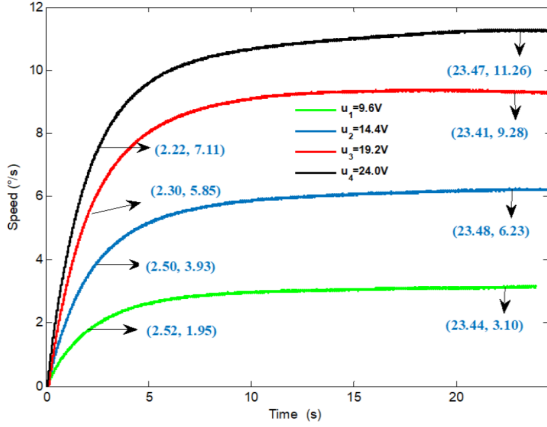


Fig. 2 The results of the MOL experiments.

Then the estimate value of parameter b should be

$$\tilde{b} = \tilde{\eta}(2)/T_s, \quad (19)$$

where $\tilde{\eta}(2)$ means the second component of $\tilde{\eta}$.

Remark: A precondition for the consistency of the above RLS method, i.e., $\lim_{t \rightarrow \infty} \tilde{\eta}_k = \eta$, is that $\sum_{k=0}^N \phi_k \phi_k^T$ is invertible. To ensure this precondition, the control input u_k should be designed reasonably. The simplest design for u_k is as follows:

$$u_k = \begin{cases} C_1 & k \leq k_0 \\ C_2 & k > k_0 \end{cases}, \quad (20)$$

where C_1 and C_2 are two different constants. A simulation for estimating parameter b will be done to evaluate the validity of the above method. The parameter setup is as follows in the simulation

$$\begin{aligned} R_a &= 2.9\Omega, & L_a &= 1.9 \times 10^{-3}H, \\ K_e &= 78V/(\text{rad s}^{-1}), & K_m &= 76\text{Nm A}^{-1}, \\ T_d &= 65.5\text{Nm}, & J &= 4000\text{kg m}^2, & T_s &= 0.001\text{s}. \end{aligned}$$

The theoretical value of b is $K_m/(JR_a) = 6.55 \times 10^{-3}$. Assign the control input u as follows:

$$u_k = \begin{cases} 10V & k \leq 500 \\ 5V & k > 500 \end{cases}. \quad (21)$$

In this situation, $\sum_{k=0}^N \phi_k \phi_k^T$ is invertible. Figure 3 shows the curves of the control input u and the estimated value of parameter b . Figure 4 shows the output angular speed v and the angular position θ . When $t_k > 0.5$ s, i.e., when u changes from 10V to 5V, the estimated value of parameter b converges to its theoretical value rapidly. The relative estimating error will be less than 2% when the simulating time t_k exceeds 0.62 s. The angular position changes less than 8° during the whole identification process. The RLS method can be used to estimate parameter b on-line with only one experiment and the process requires less time and position change than the MOL method.

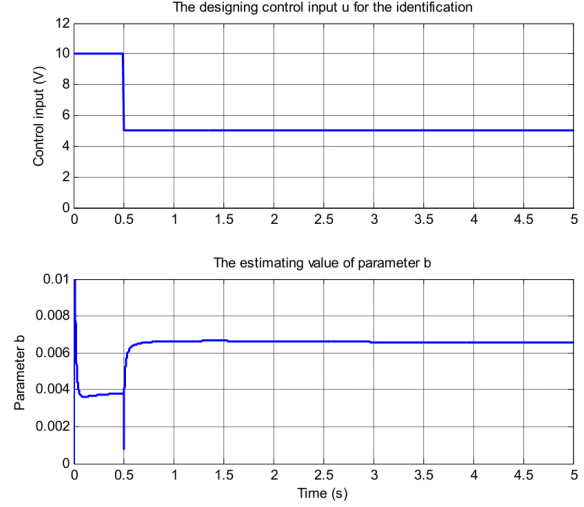


Fig. 3 The control input and the estimating of b .

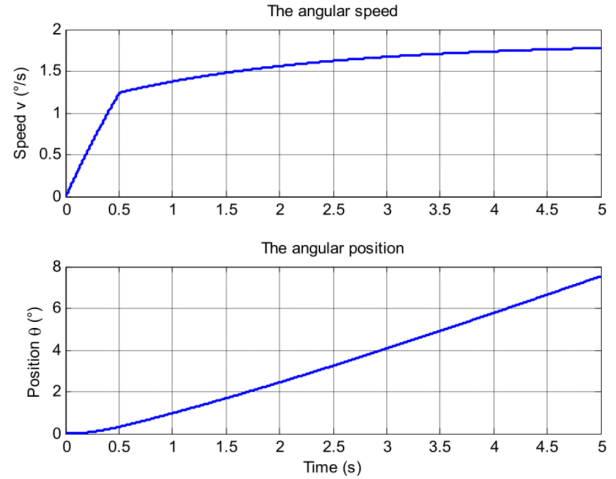


Fig. 4 The output speed and position of the system.

2.3 Speed Loop Controller Design

As the inner control loop of the main axis control, the speed loop is mainly responsible for the disturbance rejection of the system. The ADRC uses the ESO to timely estimate the total disturbances and compensates it as a feed-forward part in the controller design. It is demonstrated that the ESO can handle a large number of uncertainties in the engineering practice. Equation (3) can be generalized as

$$\dot{v} = f + b_0 u, \quad (22)$$

where b_0 is the nominal value of parameter b , f denotes the total items that affect the output except for $b_0 u$. Then the 2nd order ESO is designed as

$$\begin{cases} \dot{z}_1 = z_2 + b_0 u - 2\omega_0(z_1 - v) \\ \dot{z}_2 = -\omega_0^2(z_1 - v) \end{cases}, \quad (23)$$

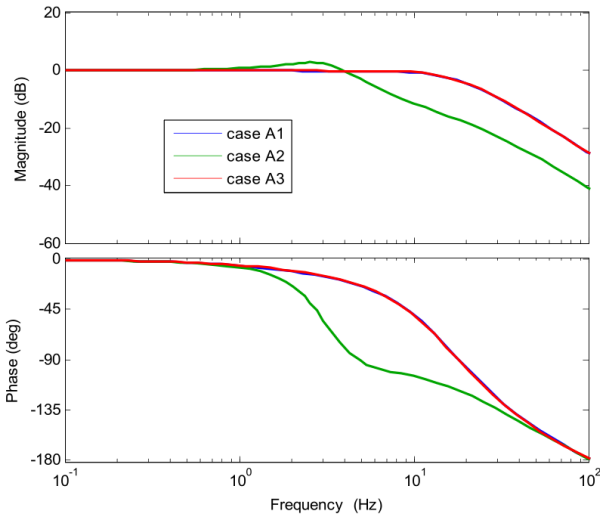


Fig. 7 Closed-loop Bode diagrams.

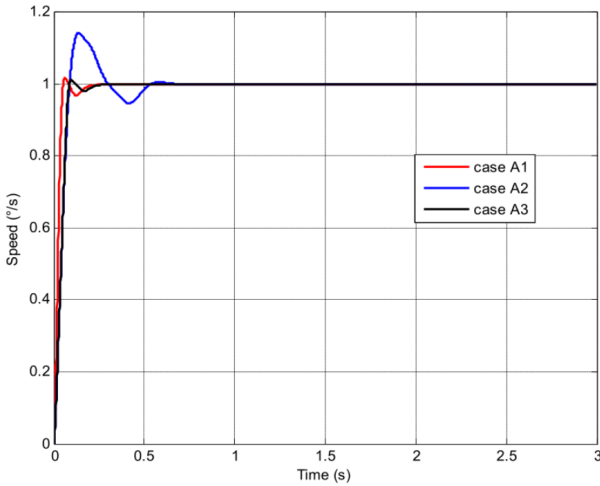


Fig. 8 The speed step responses.

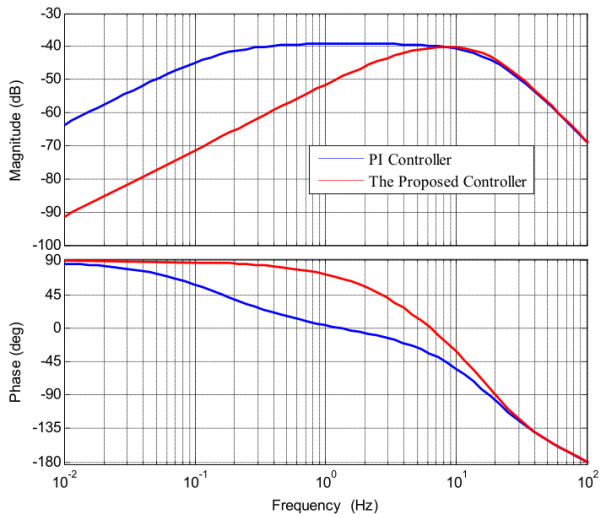


Fig. 9 Bode diagrams for the disturbance rejection.

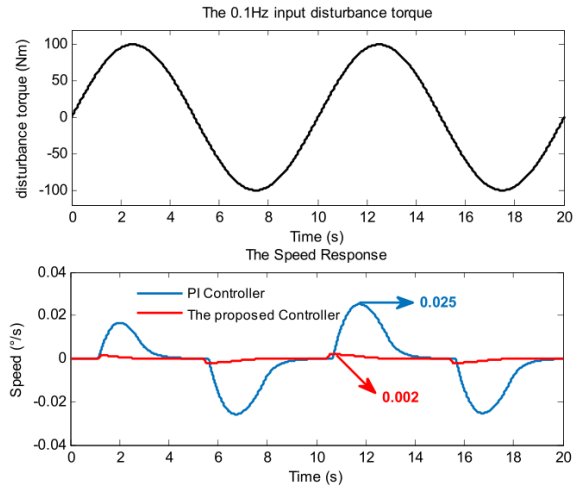


Fig. 10 Speed responses with 0.1 Hz disturbance.

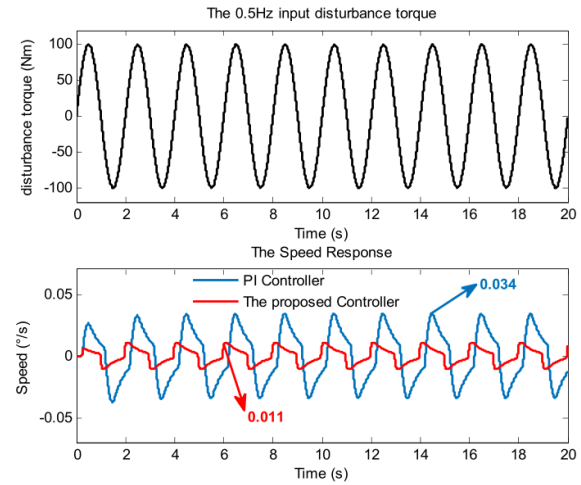


Fig. 11 Speed responses with 0.5 Hz disturbance.

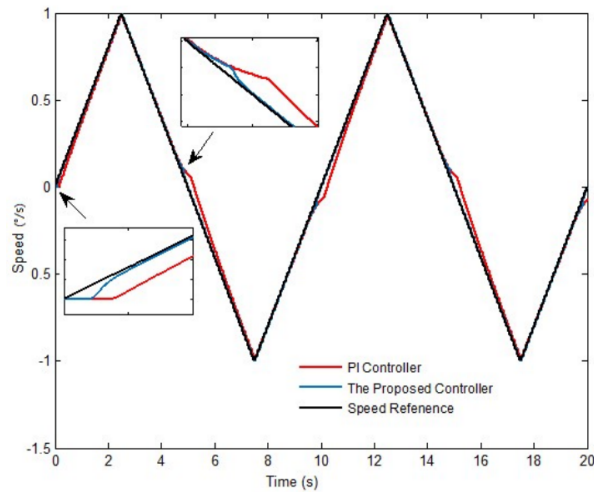


Fig. 12 Speed response of the sawtooth wave.



Fig. 13 Two design stages of the 1.2-m telescope.

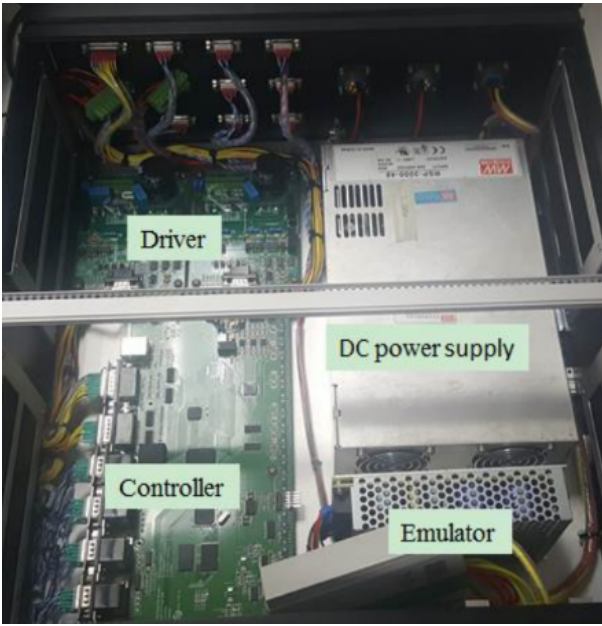


Fig. 14 Hardware platform.

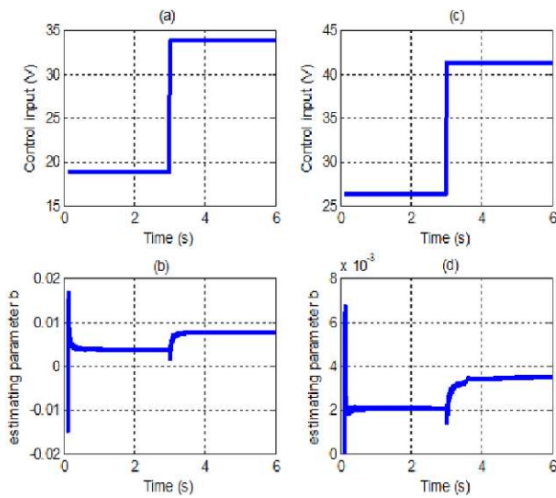


Fig. 15 Experimental results for estimating b in two stages: (a) Input voltage for the 1st stage. (b) Estimating b_0 for the 1st stage (c) Input voltage for the 2nd stage. (d) Estimating b_0 for the 2nd stage.

Let $J_1 = 1000 \text{ kg} \cdot \text{m}^2$, and $J_2 = 4000 \text{ kg} \cdot \text{m}^2$ represent the equivalent total inertia of the rotating parts in two different design stages of the telescope respectively. The other mechanical and electric parameters of the system are identical to the ones in section II. The controller parameters are designed as follows

$$\omega_0 = 40, \quad K_p = 70. \quad (28)$$

3.1 Necessity of Estimating Parameter b

The theoretical value of parameter b is 2.62×10^{-2} and 6.55×10^{-3} corresponding to the two different stages. To demonstrate the effect of the variation of parameter b , three different cases are considered

$$\begin{aligned} A1 : J = 1000, b_0 &= 2.62 \times 10^{-2}, \\ A2 : J = 4000, b_0 &= 2.62 \times 10^{-2}, \\ A3 : J = 4000, b_0 &= 6.55 \times 10^{-3}, \end{aligned} \quad (29)$$

where $A1$ and $A3$ represent the situations that $b_0 = b$, while $A2$ denotes the situation that $b_0 = 4b$. The bode diagrams of the open-loop and closed-loop transfer function are shown in Figures 6 and 7 respectively. The analysis results are summarized in Table 1. The phase margin in the open-loop bode diagram and the system bandwidth in the closed-loop bode diagram both have a remarkable reduction in case $A2$. This confirms the fact that the variation of the parameter b has a significant effect on the relative stability of the system. It also indicates the necessity for identifying parameter b when the total inertia changes significantly. Moreover, from Table 1 each index is almost the same for case $A1$ and $A3$. This means that after updating parameter b_0 , the control system will exhibit almost the same performance with the same set of control parameters even if the total inertia of the system has changed significantly.

Next, the speed responses for the three cases are analyzed. Figure 8 shows the 1° s^{-1} step response of the speed loop for the three cases, indicating that the transition process will deteriorate significantly when the parameter b_0 is not updated with its nominal value b .

The aforementioned simulation results demonstrate the necessity for updating the parameter b_0 when there is a large variation in the system for parameter b . For different design stages of the telescope, we only need to update the parameter b_0 to achieve good control performance without tuning the other control parameters. This property can significantly reduce the complexity of the controller tuning process during all the designing procedures of the telescope.

Table 1 Simulation Results in Frequency Domain

Cases	Open-loop Bandwidth (Hz)	Phase margin (°)	Closed-loop Bandwidth (Hz)	Overshoot (dB)
A1	9.3	61.9	13.7	0.0
A2	3.3	36.1	3.6	3.5
A3	9.3	60.4	13.8	0.0

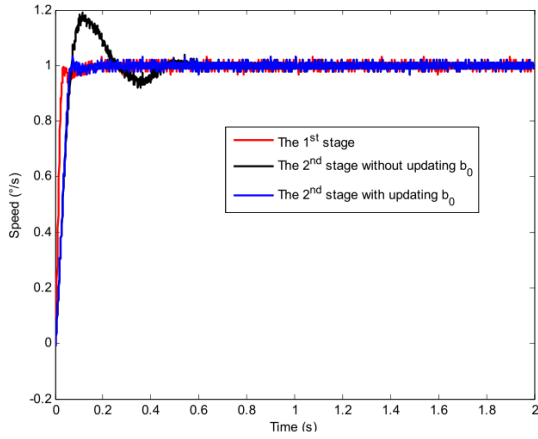


Fig. 16 The speed step responses of different stages.

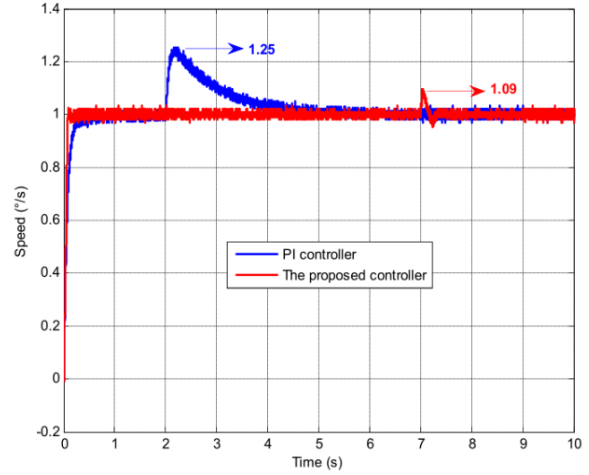


Fig. 18 Speed responses with a sudden disturbance.

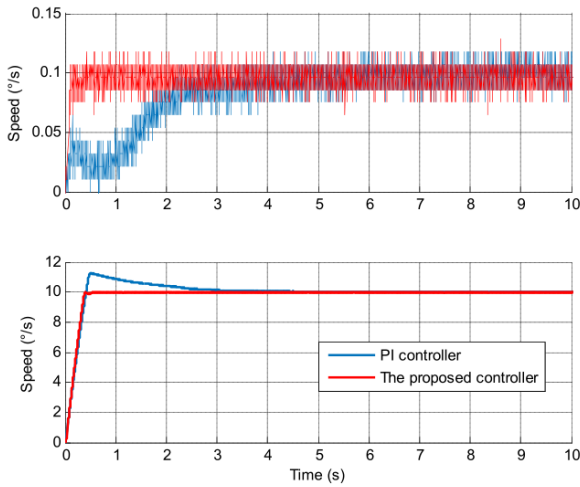


Fig. 17 Speed responses.

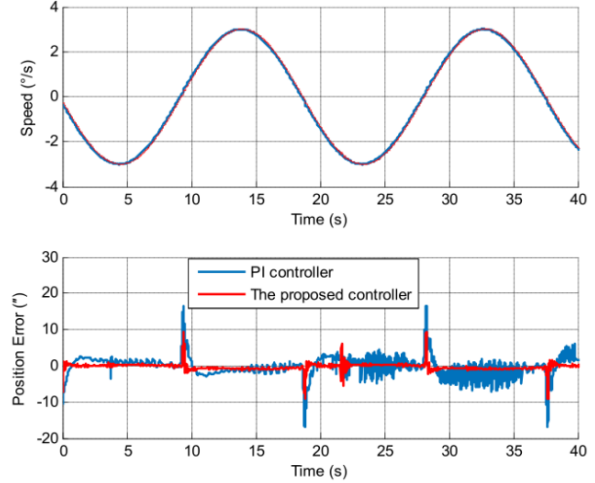


Fig. 19 Sin wave Guide position error.

3.2 Comparison with the Commonly Used PI Controller

To have an equal comparison, a PI controller is conducted on the speed loop, whose closed-loop bandwidth is also designed to be 13.7 Hz. The parameters for the PI controller are as follows:

$$K_{p_PI} = 2082, K_{I_PI} = 2483. \quad (30)$$

Figure 9 shows the comparison bode diagrams of disturbance rejection for the two controllers. Clearly, with

the same closed-loop bandwidth, the proposed controller has a distinctly better ability on disturbance rejection than the PI controller in the mid-low frequency region (0~5 Hz). The magnitude of the proposed controller is almost 25 dB lower than the PI controller at 0.1 Hz frequency. Figures 10 and 11 show the speed responses of the system with disturbance torque input at 0.1 Hz and 0.5 Hz. The magnitude of the speed fluctuation caused by the disturbance torque is reduced from $0.025^\circ \text{ s}^{-1}$ to $0.002^\circ \text{ s}^{-1}$ at 0.1 Hz and from $0.034^\circ \text{ s}^{-1}$ to $0.011^\circ \text{ s}^{-1}$ at

0.5 Hz. It confirms the fact that the proposed controller can handle the disturbance torques in the mid-low frequency region within the control bandwidth of the system. Figure 12 shows the saw tooth wave speed response of the two controllers. From the zoomed-in figures, we can see that the proposed controller has a better inhibitory effect on the static friction disturbance because it responds faster than the PI controller when the speed changes its direction.

4 EXPERIMENTS RESULTS ON THE 1.2-METER TELESCOPE

To demonstrate the effectiveness of the proposed method, several experiments were conducted during the different stages of the 1.2-m telescope design. Figure 13 shows two typical stages of the 1.2-m telescope. The experimental platform is shown in Figure 14, where the control scheme is realized based on the DSP-TMS320F28335 and FPGA-EP3C40F324 drive system. The sampling frequency of the speed loop is 1 kHz. Figure 15 shows the estimated results of the parameter b for the two stages labeled as 1st stage and 2nd stage respectively.

It indicates that the estimate parameter b_0 converges to 7.7×10^{-3} and 3.4×10^{-3} respectively. The parameter b_0 needs to be updated in the ESO design from the 1st stage to the 2nd stage. Figure 16 gives the 1° s^{-1} step responses for the two stages. It demonstrates that by updating the parameter b_0 , the speed response can still achieve good performance for the 2nd stage although the inertial of the system has changed significantly. Thus, the experiment results confirm the necessity for updating the parameter b_0 in the controller design.

Numerous experiments were conducted to compare the proposed algorithm and the commonly used PI algorithm in the 2nd stage. For an equal comparison, first, let the control input of both algorithms share the same saturation limits. Second, by regulating the parameters of the two algorithms, both closed-loop systems achieve relatively good performance with the same closed-loop bandwidth. The parameters for the two controllers are as follows

$$\begin{aligned} \omega_0 = 40, \quad K_p = 70, \quad b_0 = 3.4 \times 10^{-3}, \\ K_{p,PI} = 1735, \quad K_{I,PI} = 1978. \end{aligned} \quad (31)$$

Figure 17 gives the speed response plots of the two control methods in the low (0.1° s^{-1}) and high-speed (10° s^{-1}) conditions respectively. For the 0.1° s^{-1} step response, the rise time reduced from 2 s to 0.1 s, that is, the proposed controller can handle the static friction disturbance well at the low-speed response. For the 10° s^{-1} step response, the response time of the

proposed controller is 0.4 s without any overshoot, which is significantly faster than that of the PI controller. This confirms that the proposed controller can handle the contradiction of rapidness and overshoot perfectly at the high-speed response. Figure 18 shows the dynamic speed response of the two controllers when a sudden torque disturbance $300 \text{ N} \cdot \text{m}$ was added to the system at time point 2 s and 7 s separately. The speed fluctuation caused by the torque disturbance decreased from $0.25^\circ \text{ s}^{-1}$ to $0.09^\circ \text{ s}^{-1}$ and the adjustment time decreased from 3 s to 0.2 s. This confirms the fact that the proposed controller can handle the constant torque disturbance better than the PI controller. Figure 19 gives the comparison results of the sin-wave guide experiment. The max and RMS values of the position error reduced from $16.9''$ and $2.66''$ to $8.2''$ and $1.65''$ respectively. This confirms the fact that the proposed controller can handle the dead-zone and friction disturbance better than the PI controller.

5 CONCLUSIONS

In this paper, a RLS estimation method has been proposed which can simply estimate the parameter on line. A simplified 2nd order ESO and the simplest proportional controller have been employed to guarantee the performance of the closed-loop system. In summary, the proposed controller has the following advantages.

(i) Only two parameters need to be tuned when the situation is not changed significantly. It is as easy as the PI controller, which makes it favorable in the engineering practice.

(ii) Only one parameter needs to be updated once the inertia of the plant changes remarkably. The new estimating value of the parameter can be obtained online.

(iii) Using the same set of control parameters we can obtain good control performance in a significant range of speed variations.

The method can compensate for the static friction effectively in the extremely low-speed response and can avoid the overshoot phenomenon in the high-speed response. The simulation and experimental results have demonstrated that the proposed control algorithm displays good control performance even if the operating conditions change significantly.

Acknowledgements This work was supported in part by the National Natural Science Foundation of China (Grant Nos. 12122304 and 11973041), and in part by the Youth Innovation Promotion Association CAS (No. 2019218).

References

- Alonge, F., Cirrincione, M., D'Ippolito, F., Pucci, M., & Sferlazza, A. 2017, *IEEE Trans. Ind. Electron.*, 64, 5608
- Ang, K. H., Chong, G., & Li, Y. 2005, *IEEE Trans. Control. Syst. Technol.*, 13, 559
- Back, J., & Kim, J. 2015, *International Journal of Robust and Nonlinear Control*, 25, 2254
- Chang, X., Li, Y., Zhang, W., Wang, N., & Xue, W. 2015, *IEEE Trans. Ind. Electron.*, 62, 991
- Chen, S., Hung, Y., & Gong, S. 2016, *Int. J. Fuzzy Syst.*, 18, 1065
- Gao, Z. 2003, in *Proceedings of the 2003 American Control Conference*, 2003., 6, 4989
- Han, J. 2009, *IEEE Trans. Ind. Electron.*, 56, 900
- Huang, Y., & Xue, W. C. 2014, *ISA Trans*, 53, 963
- Hui, J., Ge, S., Ling, J., & Yuan, J. 2020, *Annals of Nuclear Energy*, 143, 107417
- Jafarov, E. M., Parlakci, M., & Istefanopulos, Y. 2005, *IEEE Transactions on Control Systems Technology*, 13, 122
- Liu, J., Sun, M., Chen, Z., & Sun, Q. 2019, *Aerospace Science and Technology*, 95, 105468
- Rigatos, G. G. 2009, *Electric Power Systems Research*, 79, 1579
- Shi, D., Xue, J., Zhao, L., Wang, J., & Huang, Y. 2017, *IEEE/ASME Transactions on Mechatronics*, 22, 2277
- Song, X.-L., Wang, D.-X., & Zhou, W.-P. 2021, *RAA (Research in Astronomy and Astrophysics)*, 21, 163
- Wang, Q., Cai, H.-X., Huang, Y.-M., et al. 2016, *RAA (Research in Astronomy and Astrophysics)*, 16, 007
- Wu, Z., Li, D., Xue, Y., et al. 2020, *ISA Transactions*, 102, 135
- Wu, D., & Chen, K. 2009, *IEEE Transactions on Industrial Electronics*, 56, 2746
- Xia, Y., Fu, M., Li, C., Fan, P., & Xu, Y. 2018, *IEEE Transactions on Industrial Electronics*, 65, 4051
- Xia, X., Zhang, B., Li, X., & Zhang, S. 2019, *Guangxue Jingmi Gongcheng/Optics and Precision Engineering*, 27, 2628 (in Chinese)
- Xue, W., Bai, W., Yang, S., et al. 2015, *IEEE Transactions on Industrial Electronics*, 62, 5847
- Yao, S., Gao, G., Gao, Z., & Li, S. 2020, *ISA Transactions*, 101, 327
- Yuan, Y., Yu, Y., Wang, Z., & Guo, L. 2019, *IEEE Transactions on Industrial Electronics*, 66, 4608